Pergamon

Cement and Concrete Research, Vol. 25, No. 3, pp. 658-670, 1995

0008-8846/95 $9.50+.00

0008-8846(95)00054-2

HIGH-CALCIUM COAL COMBUSTION BY-PRODUCTS: ENGINEERING PROPERTIES, ETTRINGITE FORMATION, AND POTENTIAL APPLICATION IN SOLIDIFICATION AND STABILIZATION OF SELENIUM AND BORON

J.K. Solem-Tishmack* and G.J. McCarthy
Department of Chemistry
North Dakota State University
Fargo, ND 58105

B. Docktor, K.E. Eylands, J.S. Thompson and D.J. Hassett
Energy and Environmental Research Center
University of North Dakota
Grand Forks, ND 58202

(Refereed)
(Received June 2, 1994; in final form January 9, 1995)

ABSTRACT

Four high-calcium coal combustion by-products (two pulverized coal fly ashes (PCFA), a flue gas desulfurization (FGD) residue, and an atmospheric fluidized bed combustion (AFBC) fly ash), were tested for engineering properties and ability to immobilize boron and selenium. These data are needed to explore high-volume utilization in engineered structures or in solidification/stabilization (S/S) technology. Strengths of cured pastes (91 days), varied from as much as 27 MPa (3900 psi) for one of the PCFA specimens to 4.6 MPa (670 psi) for the FGD specimen. All of the coal by-product pastes developed more than the 0.34 MPa (50 psi) required for S/S applications. Ettringite formation is important to engineering properties and S/S mechanisms. XRD on plain specimens cured for 91 days indicated that the two PCFA pastes formed 5-6% ettringite, the FGD paste formed 22%, and the AFBC paste formed 32%. The hydrating PCFA pastes showed little expansion, the FGD paste contracted slightly, and the AFBC paste expanded by 2.9% over 91 days. Se and B were spiked into the mixing water as sodium selenite, selenate and borate, and for most pastes this had little effect on strength, workability, and expansion. Leaching of ground specimens (cured for 91 days) showed a generally positive correlation between the amount of ettringite formed and resistance to Se and B leaching. Se spiked as selenate was more readily leached than Se spiked as selenite. B showed a high level of fixation.

Introduction

High-calcium coal combustion by-products (CCBP) are typically cementitious, due principally to the formation of ettringite (nominally $Ca_6Al_2(SO_4)_3(OH)_{12}\cdot 26H_2O$). Ettringite forms

*Present address: School of Civil Engineering, Purdue University, West Lafayette, IN 47907.

in coal by-products that contain high levels of calcium and sulfate, react with water to give pH above *ca.* 12, and include aluminum that can be solubilized at high pH. These conditions are met by high-calcium pulverized coal fly ashes (PCFA), by residues from some of the newer "clean coal" technologies, and by some flue glass desulfurization (FGD) residues.

Previous research on co-disposal of high-calcium by-products from gasification and combustion of North Dakota lignite (1-5) showed that the hydrated solids had reduced leachability of trace elements such as As, Se and B. The principal hydration product was ettringite, and it was inferred that this phase was responsible for immobilization of the trace elements in oxyanion form. It is known that numerous oxyanions can be incorporated into the ettringite structure (5-11). The combination of cementitious properties and the potential for immobilization of hazardous trace elements could result in utilization of these high-calcium CCBP in engineered structures and materials, and in solidification/stabilization (S/S) technology (12-18).

For ten representative CCBP, Solem and McCarthy (19) recently studied the hydration behavior and the extent of ettringite formation as a function of water to solid ratio (w/s) and curing time. After 91 days of curing, pulverized coal fly ashes formed relatively small amounts (6-10%) of ettringite because of insufficient sulfate. For CCBP richer in soluble sulfate, ettringite formation ranged from 15% to 30%. Four of the CCBP were selected for the present study, objectives of which were to evaluate: workability of pastes; extent of ettringite formation; crystal morphology and microstructure; strength of the solidified pastes; expansion during curing (potentially from the formation of ettringite); and leachability of two potentially hazardous elements, Se and B, in cured pastes.

Experimental

Materials

Chemical compositions and crystalline phases relevant to hydration reactions for the four high-calcium coal combustion by-products are given in Table 1. Each material is discussed briefly below. Additional characterization of these materials is given by Solem and McCarthy (19) and Solem-Tishmack (20).

WY FA. A high-calcium PCFA from a power plant in Nebraska that burns Wyoming (Powder River Basin) subbituminous coal. This distinctly cementitious material, which is marketed in the Midwestern U.S., is typical of high-calcium fly ashes (21). It has a low sulfate concentration which limits its ettringite formation (19). Its crystalline phases relevant to hydration reactions are anhydrite ($CaSO_4$), lime (CaO), and C_3A ($Ca_6Al_2O_6$). It also contains quartz (SiO_2), mullite ($Al_6Si_2O_{13}$), ferrite spinel ($(Fe,Mg)(Fe,Al)_2O_4$), melilite ($Ca_2(Mg,Al)(Al,Si)_2O_7$), merwinite ($Ca_2Mg(SiO_4)_2$) and periclase (MgO) (21), which are largely unreactive in cementitious systems.

ND FA. A North Dakota lignite PCFA that is utilized commercially in concrete. This is a low-sodium ash that develops strength slowly as a paste (19), but is an effective pozzolan in blended cement. This ash has small amounts of anhydrite and C_3A in addition to quartz, ferrite spinel, periclase and merwinite (21).

MN FGD. A flue gas desulfurization residue from a power plant in Minnesota that burns Montana subbituminous coal. This plant uses a dry scrubber process that results in calcium sulfite hemihydrate (hannebachite), instead of the more common calcium sulfate dihydrate (gypsum), as the scrubber residual. This material is a composite of subbituminous coal fly ash, sorbent product (sulfite) and a small amount of unreacted sorbent (CH). Hannebachite is

TABLE 1. Chemical and Mineralogical Compositions

CCBP	Chemical Composition[a] (weight percent)										XRD Mineralogy[b]
	SiO_2	Al_2O_3	Fe_2O_3	CaO	SO_3	MgO	Na_2O	K_2O	H_2O^c	LOI[d]	
WY FA	33.8	18.7	4.8	26.5	1.8	5.4	2.04	0.36	0.03	0.33	Anhydrite, C_3A, Lime
ND FA	46.0	14.5	6.7	17.9	1.4	5.1	1.16	1.86	0.01	0.02	Anhydrite, C_3A
MN FGD	32.0	15.3	3.8	24.1	13.0	2.9	1.67	0.52	0.55	1.41	Hannebachite, CH
KY AFBC	12.3	4.0	9.5	41.4	15.2	2.4	0.07	0.55	0.24	10.80	Lime, CH, Anhydrite

a. H_2O = moisture content; LOI = loss on ignition.
b. XRD mineralogy relevant to cementitious reactions: Anhydrite = $CaSO_4$; C_3A = $Ca_3Al_2O_6$; CH = $Ca(OH)_2$; Hannebachite = $CaSO_3 \cdot 0.5H_2O$; Lime = CaO.
c. 110°C.
d. 800°C.

relevant to cementitious reactions because it is the sulfite (and/or sulfate) source for ettringite reactions (5,19).

KY AFBC. An atmospheric fluidized bed combustion fly ash from a power plant in Kentucky that uses a bituminous coal source. Some char is included with the fly ash. The material has a high Ca and sulfate content and a low Al content. Its major crystalline phases are lime, CH and anhydrite. The CH formed from the "soft-burned" lime on contact with moist air. This CCBP also contains quartz, hematite and a small amount of periclase.

Methods

Fabrication and Formulation of Test Specimens. Standard American Society for Testing and Materials (ASTM) methods (22) were used for fabrication and testing: CCBP-water mixing, ASTM C305; paste flow determination, ASTM C230; paste curing, ASTM C511; mortar bar preparation, ASTM C151. Pastes of neat by-products were fabricated into cubes and cured for 7, 28, and 91 days (d). Along with plain paste, additional pastes spiked with Se or B were also prepared. Although the CCBP already contained some Se and B, additional amounts of these elements in the form of sodium selenite, sodium selenate, and sodium borate were added to the mixing water. The level of spiking was dictated by the need to choose a concentration high enough to be detectable by the analytical methods at the 1% leaching level, without consideration of the Se and B already present.

There were only three 51 mm (2") cubes and two 25x25x305 mm (1"x1"x12") prisms fabricated for each paste, due to limitations in the quantity of available material. The cubes and prisms for the plain pastes were unmolded after 24 h. The mortar bars proved to be fragile, and several of them were broken in handling. The Se- and B-spiked pastes were kept in the molds for an additional 24 h.

XRD. Qualitative and semi-quantitative XRD analyses were performed at all sampling times. The amounts of ettringite and other relevant phases formed by hydration reactions were quantified by methods described by Thedchanamoorthy and McCarthy (23,24), and revised by Bender et al. (25-27) for ettringite, anhydrite, lime, gypsum, portlandite and hannebachite.

SEM. Microstructures of the cured pastes were examined on carbon-coated fracture surfaces. EDX spectrometry was employed as an aid in identifying the chemical composition of some crystals and matrices.

Flow Table. A Flow Table (ASTM C-230) was used to evaluate the workability of pastes. The flow of the paste was tested immediately after mixing. A percent flow of 90% to 120%, typical for most blended cements, was chosen as a target range for the pastes. The approximate w/s ratios were determined by trial and error.

Unconfined Compressive Strength and Length Changes. The compressive strength was determined according to ASTM C-109 using 51 mm (2") cube specimens. The compressive strength measurements were taken on one cube at each of the three curing times. Some of the cubes were not perfectly regular due to the difficultly encountered in molding (MN FGD paste) or expansion of the paste (KY AFBC) during curing. Since only a single specimen was tested and some of the specimens were slightly deformed, the data are presented for general information, but no conclusions are drawn. Length changes were measured with a Length Comparator, described in ASTM C-490, using the 25x25x305 mm prisms. In some specimens, one or both of the prisms broke, either during unmolding or during the first measurement, leaving only one measurement of expansion for that specimen. The remaining length change data are average values for two measurements. Length changes (expansion or contraction) were reported to the nearest $\pm 0.01\%$.

Leaching Procedure. After 91 d curing, a batch extraction test modeled after the U.S. Environmental Protection Agency's Toxic Characteristic Leaching Procedure (TCLP) (28), but using deionized water as the leachant (28), was performed on a portion of the cube tested for unconfined compressive strength. The specimen was ground to give a particle size similar to that required for the TCLP (<0.3 mm). Five grams of the powder were placed in a 200 mL plastic bottle, along with 100 mL of deionized water. The mixture was shaken and placed on a rotator that inverted the bottles at 45 rpm, for 18 h. Grinding the hardened pastes enhances access of leachant to the total mass of solid, so that the leaching test assesses atomic-scale immobilization rather than just physical encapsulation of the Se and B. The solution was filtered and analyzed for Se and B by inductively coupled argon plasma spectroscopy.

Results and Discussion

Table 2 summarizes the engineering properties determined for the plain and spiked pastes at various curing times. Characterization of hydrated pastes by XRD and SEM will be presented first to provide a context for discussion of the physical properties.

Mineralogy and Microstructure

Ettringite was observed in all specimens. Figure 1 gives portions of the X-ray diffractograms of the four specimens cured for 91 d, and Figure 2 shows selected microstructural features. The amount of ettringite formed after 7, 28 and 91 d curing is given in Table 2. Much of the fly ash was unreacted as noted by the presence of amorphous "humps" in the X-ray diffractograms (Fig. 1) and the spherical fly ash grains in the SEM micrographs (Figs. 2a and 2c).

WY FA. In addition to ettringite, strätlingite (gehlenite hydrate, $Ca_2Al_2SiO_7 \cdot 8H_2O$) and calcium monosulfoaluminate hydrate (AFm, nominally $Ca_4Al_2SO_4(OH)_{12} \cdot 6H_2O$) were observed by XRD (Fig. 1a). The appearance of these Ca-Al-rich phases indicates sulfate depletion of pore solutions. The SEM micrograph (Fig. 2a) shows a region of platy crystals, prominent interconnections among fly ash grains, and small knobs covering the surface of fly ash grains. Other areas of the specimens showed features such as a dense microstructure and well

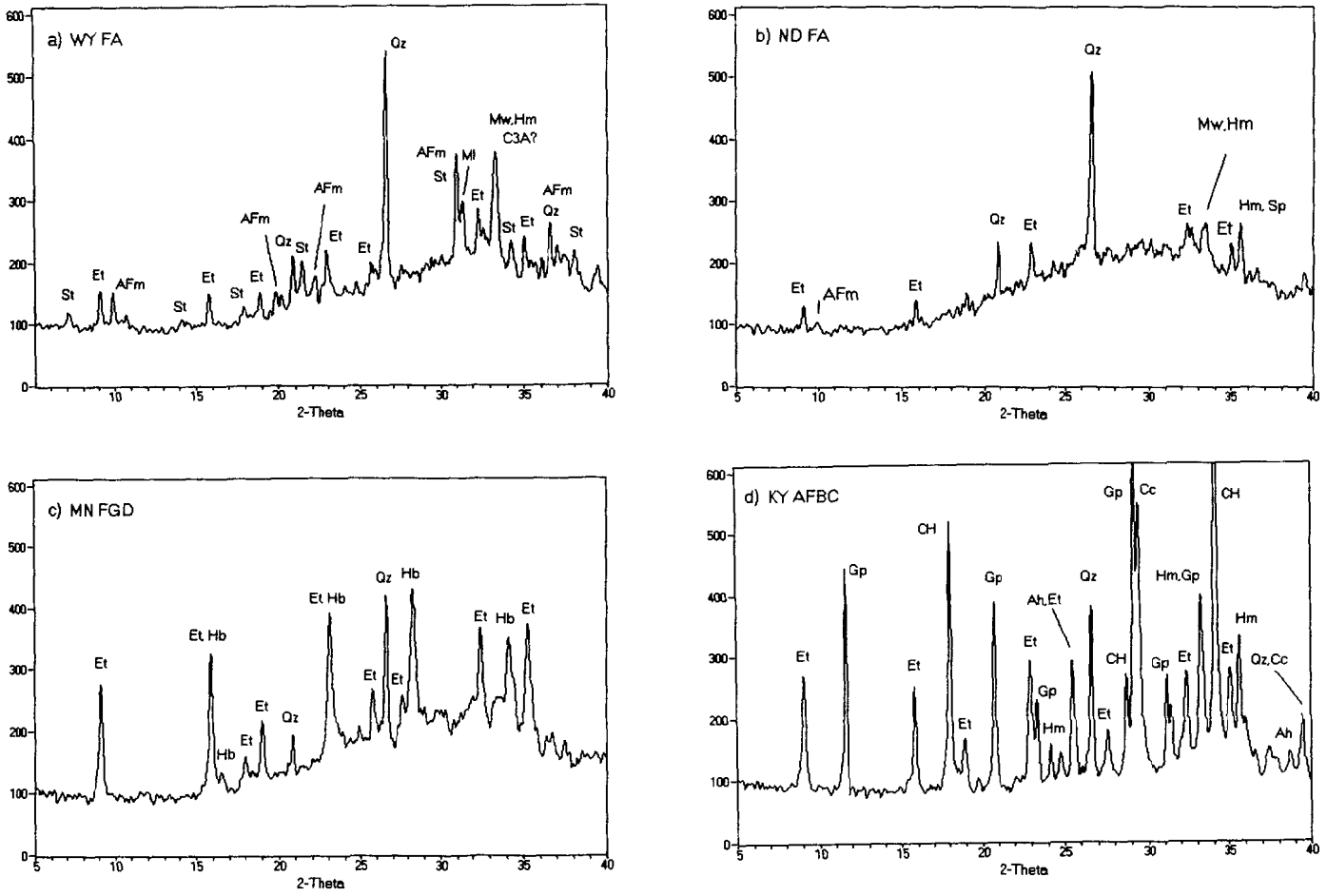

FIG. 1. X-ray diffractograms (CuKα radiation; intensity in c/s) of the four CCBP after curing for 91 d. AFm = calcium monosulfoaluminate hydrate; Ah = anhydrite; Cc = calcite; CH = $Ca(OH)_2$; C_3A = $Ca_3Al_2O_6$; Et = ettringite; Gp = gypsum; Hb = hannebachite; Hm = hematite; Ml = melilite; Mw = merwinite; Qz = quartz; St = strätlingite.

TABLE 2. Engineering Test Results and Ettringite Formation

CCBP Spike	% Flow	Expansion %			Compressive Strength (MPa)			Ettringite %		
		7d	28d	91d	7d	28d	91d	7d	28d	91d
WY FA (w/s = 0.25; 80% ash)										
plain	125	-0.00	-0.00	0.00	22	26	27	7	6	6
selenite	121	-0.00	0.01	0.01	21	19	26	7	9	8
selenate	120	-0.00	0.01	0.01	33	30	22	7	7	4
borate	103	0.02	0.04	0.05	21	25	31	15	12	11
ND FA (w/s = 0.17; 86% ash)										
plain	97	-0.01	-0.01	0.01	3.9	4.1	13	6	6	5
selenite	100	-0.00	-0.01	0.00	4.3	4.4	14	7	7	6
selenate	100	NA*	NA	NA	3.0	5.2	8.4	4	9	6
borate	96	0.02	0.02	0.04	5.2	6.4	28	7	7	6
MN FGD (w/s = 0.45; 69% ash)										
plain	83	-0.09	-0.11	-0.12	1.6	2.9	4.6	20	19	22
selenite	92	NA	NA	NA	1.8	2.8	-	20	18	-
selenate	89	NA	NA	NA	1.9	4.2	4.5	22	22	21
borate	96	-0.01	-0.03	0.01	3.8	5.0	5.8	21	27	26
KY AFBC FA (w/s = 0.45; 69% ash)										
plain	101	0.42	1.20	2.86	3.6	7.7	8.5	15	20	32
selenite	113	NA	NA	NA	2.5	6.0	9.3	11	21	28
selenate	107	0.29	1.13	2.66	2.0	5.9	10	12	21	21
borate	99	0.13	0.36	2.88	1.5	4.0	7.3	12	27	33

*NA = specimen not available

developed laths (ettringite). The corresponding B-spiked specimens (not shown) contained very fine featherlike platelets that were much thinner and more numerous than the previously mentioned platy crystals. The B-spiked paste also had almost twice the ettringite of the plain paste.

ND FA. Ettringite and calcium monosulfoaluminate hydrate were the crystalline hydration products (Fig. 1b). Surface reaction was observed on fly ash grains by SEM (Fig. 2b). The corresponding B-spiked specimen (not shown) showed a large amount of bridging between fly ash grains, a microstructural feature consistent with the increase in strength measured for this sample. The B-spiked sample also contained some platy crystals.

MN FGD. An ettringite structure phase was the only crystalline hydration product identified by XRD (Fig. 1c). This phase may be a sulfite rather than a sulfate. Pure sulfite ettringite is readily synthesized (4,6,10,18) and the stronger peaks in X-ray diffractograms are so similar to those of sulfate ettringite that these cannot be readily distinguished (10,18). Some hannebachite was still prominent in the diffractograms, demonstrating its slow rate of oxidation in air to sulfate. SEM micrographs show small knobs covering the FA grains, (Fig. 2c) and little bridging between fly ash grains. Shrinkage cracks were also observed.

KY AFBC. These specimens had the greatest ettringite contents. This observation is notable in light of the low Al_2O_3 content of this CCBP (4.0%; Table 1). In these materials, a given mass of soluble alumina can produce *ca.* 12 times its mass of ettringite if sufficient CaO,

FIG. 2a
SEM micrograph of the WY FA after 7 d curing.

FIG. 2b
SEM micrograph of the ND FA after 28 d curing.

FIG. 2c
SEM micrograph of the MN FGD after 28 d curing.

FIG. 2d
SEM micrograph of the KY AFBC after 28 d curing.

SO_3 and H_2O are available. XRD showed that gypsum and portlandite were also abundant and some anhydrite remained after 91 d. In the SEM micrograph (Fig. 2d), rod-shaped crystals (ettringite), bladed crystals (gypsum) and platy crystals (CH) were all prominent. Several micrographs (not shown) revealed the presence of highly etched crystals of anhydrite, suggesting slow reaction with pore solutions. Calcite, formed presumably as a result of exposure of CH to atmospheric carbon dioxide, was also observed.

Some C-S-H or C-A-S-H gel formation in these CCBP is likely (30), but no direct evidence was found in either the X-ray diffractograms or SEM micrographs.

Percent Flow and Workability of the Pastes

WY FA. A w/s ratio of 0.25 was selected from preliminary trials with plain WY FA. The

percent flow was similar for three of the pastes (120-125%), but deviated from this range in the B-spiked paste (103%). There were also differences in the amount of ettringite formation and expansion in this B-spiked paste.

ND FA. All four pastes, made at w/s = 0.17, had a similar percent flow (96-100%).

MN FGD. A workable plain paste was obtained at a w/s = 0.45. The percent flow of the four pastes ranged from 83% to 96%. The physical properties of this paste were very different from the other high-calcium CCBP. The rheology of the MN FGD is controlled by the combination of spherical pulverized coal fly ash grains and platy sorbent material. The fly ash grains gave the pastes some of the rheological properties of the WY and ND FA pastes, but the sorbent particles (although they had low reactivity) promoted high water demand. This paste had a stronger surface tension than the other high-calcium CCBP. The surface tension made it difficult to force the paste all the way into the corners of the mold, and some of the cubes were deformed. The MN FGD took longer to harden than did the other specimens.

KY AFBC. At w/s = 0.45, the percent flow of the four pastes ranged from 99% to 113%. Although the KY AFBC had a reasonably high percent flow, the paste was the most difficult to mold. The paste stiffened markedly in the few minutes needed for mixing, flow testing and molding. The exothermic reaction of lime hydrating to CH generated enough heat to require gloves to handle the molds.

The flow measured for each paste was not necessarily a good indication of its workability, defined here as the relative ease or difficulty of molding the paste. Among the factors that affect workability of the hydrated solids are the shapes of the particles and their chemical reactivity. The presence of blocky, irregularly shaped sorbent materials (reacted and unreacted) in the MN FGD and KY AFBC pastes increased water requirements and reduced flow compared to the PCFA pastes, with their high content of spherical particles. The high reactivity of the AFBC paste was noted above. The Flow Table measurements were helpful, however, in evaluating whether or not the addition of a spiked solution had any effect on the workability of the paste. With the exception of the WY FA borate paste, there were no significant changes in the flow that could be attributed to the presence of a spiked solution.

Unconfined Compressive Strength

As indicated in Table 2, the WY FA plain paste specimen developed 27 MPa (3900 psi) after 91 d, the greatest value of the specimens. An specimen cured for only 7 d developed 22 MPa (3200 psi), suggesting that early strength gain is characteristic of this material. In contrast, the weakest specimen, MN FGD, developed only 4.6 MPa (670 psi) at 91 d. The KY AFBC plain paste specimen developed 8.5 MPa (1300 psi), with most of the strength gain occurring between 7 and 28 d. Thus these materials are highly variable in the type of strength developed.

A particularly noteworthy comparison is between the results for ND FA plain and B-spiked values. The latter specimen showed a much higher strength value. The results of the strength test are consistent with the microstructural observations of greater bridging developed between particles in the B-spiked specimen. Adding salts to mixing water can affect cementitious properties such as strength development, setting times, and drying shrinkages (31). Because of the low mass of B, sodium borate additions gave this paste a high salt concentration in its mix water (2753 mg/L B and 2932 mg/L Na). Borates are known to retard the set time (30), but

are not known to give late strength gain. The high Na concentration may have enhanced pozzolanic reactions in this fly ash.

Length Changes and Ettringite Formation

The WY and ND FA specimens formed less than 10% ettringite and showed only a slight contraction or expansion (0.01% or less) (Table 2). Slightly higher values were observed in the WY FA B-spiked specimen. The MN FGD plain specimens formed approximately 20% ettringite and yet contracted over the 91 d curing (-0.09 after 7 d and -0.12% after 91 d). No length measurements were available for the selenate or selenite specimens due to breakage of the mortar bars and the B-spiked specimen expanded slightly over the 91 d curing. The KY AFBC specimens formed 30% ettringite and exhibited the greatest expansion in the study (about 2.8% after 91 d). All the lime in these pastes had hydrated to portlandite within the first 24 h and was not responsible for expansion after that time. Unlike the other CCBP, a significant amount of the total ettringite formed between 28 and 91 d. Significant expansion in hydrated KY AFBC by-products has also been observed in other studies (30).

The mechanism of sulfate-induced expansion and ettringite formation still remains unclear. Evidence presented in the literature and reviewed by Mehta (32,33), Cohen (34), and Ping and Beaudoin (35,36) suggests that expansion (and strength gain) resulting from ettringite formation relates more to the environment in which it forms. Lime content, the pH, an external source of water or sulfate-rich water, and physical confinement are all factors that influence the size and morphology of ettringite and the amount of expansion in a cementitious system. The conditions are apparently favorable for paste expansion of this AFBC material.

Although the KY AFBC specimens showed expansion between 7 and 91 d, their strength also increased during this time period. Latent ettringite formation in concrete usually contributes to both expansion and strength loss. Apparently, the expansion behavior in hydrated CCBP pastes cannot be compared directly with conventional portland cement systems, because the cementation mechanisms sulfo-pozzolanic *vs.* silico-pozzolanic binders (30) differ so greatly.

Leachability of Selenium and Boron

The concentrations of Se and B in the plain and spiked CCBP, and the results of the leaching tests, are given in Table 3. The amount of Se added was much higher than what was initial-

TABLE 3. Concentration of Se and B in the CCBP Before and After Spiking, and and Results of the Leaching Tests.

CCBP	Original CCBP		Total after Spiking		Leachate Concentration			Percent Leached		
	Se	B	Se	B	Se Selenite Spike	Se Selenate Spike	B Borate Spike	Se Selenite Spike	Se Selenate Spike	B Borate Spike
	mg/kg				mg/L			%		
WY FA	12.5	1232	413	2032	0.64	2.20	1.40	6.2	21	2.8
ND FA	13.7	1829	414	2629	0.18	2.60	2.40	1.7	25	3.7
MN FGD	7.6	1352	408	2152	--	0.65	0.49	---	6.4	0.9
KY AFBC	7.7	441	408	1241	0.04	2.90	0.25	0.4	29	0.8

ly present in the specimens, but the amount of B in the CCBP was already much greater than the spike. Calculations of percent leached used total Se and B.

WY FA. For the paste spiked with selenite, 6.2% of the total Se was leached (94% was immobile). When the Se spike was in the form of selenate, 21% was leached. Only 2.8% of the total B was leached.

ND FA. This PCFA paste performed similarly to the WY FA paste: 1.7% Se leached from the selenite-spiked paste, but 25% leached from the selenate-spiked paste; 3.7% of the total B was leached.

MN FGD. This had the lowest Se leachability (6.4%) of the four selenate-spiked pastes. The selenite specimen was not available for testing. Only 0.9% of the B was leached.

KY AFBC. This had the lowest Se leachability among the selenite-spiked pastes (0.4%), but the highest Se leachability when the Se-spike was in the form of selenate. The B leachability was very low (0.8%).

With one notable exception, the pastes that formed the most ettringite had the lowest Se and B leachabilities. The B leachabilities were low with all four high-calcium CCBP pastes. The results in Table 3 indicate a trend of increased leachability when Se is speciated as selenate rather than selenite. It may be due to an ettringite structural control, namely that during crystallization, selenite (SeO_3^{2-}) is more competitive for the sulfate sites than is selenate (SeO_4^{2-}). One CCBP paste, MN FGD, showed a four-fold improvement in Se-as-selenate fixation. Here the dominant solid phase is calcium sulfite hemihydrate (hannebachite). The ettringite structure hydration product is believed to be selenite-ettringite. Selenate may be incorporated more readily into the ettringite structure when the sulfate source is limited and/or the competing oxyanion is sulfite rather than sulfate.

Resource Conservation and Recovery Act (RCRA) regulations defining a hazardous waste stipulate that leachates from the EP Test for Toxicity or TCLP must not contain more than 1.0 mg/L of Se (28,37). Presently, B is not regulated for drinking water, but concentrations exceeding 2 mg/L are considered toxic for plants (38). When the Se was spiked as selenite, the three CCBP pastes tested had leachabilities below hazardous level according to the RCRA 1.0 mg/L criterion (Table 3). However, three of the four selenate-spiked pastes have Se leachabilities 2 to 3 times above this level. This result indicates that in any evaluation of the hazardousness of a CCBP product used in solidification/stabilization (S/S) technology, the speciation of Se in Se-containing wastes and the redox conditions of leaching tests and disposal areas must be considered.

The B-spiked ND FA paste slightly exceeded the irrigation standard of 2 mg/L. This material contained the largest amount of total B (Table 3). The B in the other three CCBP pastes cured for 91 d was sufficiently immobile, especially when abundant ettringite crystallized, that these pastes readily passed the irrigation standard.

Application of High-Calcium Coal Combustion By-Products to Engineered Structures and Materials

The cementitious nature of CCBP suggests that they could be employed in such as high-volume engineered structures highway sub-bases, embankments, backfills, or even construction

materials such as bricks. The four CCBP studied here have many desirable characteristics, provided that allowance is made for the contraction or expansion on curing. However, it should be cautioned that the long-term environmental stability of ettringite-based sulfo-pozzolanic binders is of concern, as emphasized by Berry et al. (30). As with many phases in cementitious materials, ettringite is not thermodynamically stable (39) in contact with aqueous solutions at near-neutral, or lower, pH. The long-term "kinetic stability" (durability) of ettringite-based sulfo-pozzolanic binders under more neutral aqueous solutions, such as rain water and ground water, is suspect. There are reports that atmospheres rich in CO_2 can degrade pure synthetic ettringite in a matter of weeks (40,41)). In long-term field tests of several types of CCBP emplaced in instrumented test cells (27,42-44), we have found that ettringite has survived leaching by rain water and ground water for up to five years, but matrix phases associated with it (portlandite, gypsum, calcite, C-S-H, etc.) have been replaced by thaumasite (nominally $Ca_3[Si(OH)_6]SO_4CO_3 \cdot 12H_2O$). Cores from these monofills, which had good strength and low permeability when emplaced, had lost more than 90% of that strength and increased by up to 10^2 in permeability after thaumasite formation (42). Clearly, the long-term durability of sulfo-pozzolanic binders needs further study.

Application of High-Calcium Coal Combustion By-Products to S/S Technology

The principal advantage in developing S/S technologies that employ CCBP is to make use of an industrial by-product that lowers the costs of the S/S technology, and saves disposal costs for the generator of the CCBP. All of the CCBP pastes developed enough strength to meet the required 50 psi for use in S/S technology (37), although the strength development observed here could be significantly different when hazardous waste solids or liquids are included in the pastes. With the exception of the potentially undesirable exothermic AFBC hydration reaction, the fabrication of pastes was straightforward. The AFBC paste expanded sufficiently on curing that its physical integrity in a confined container would be of concern. The generally low Se and B leachabilities of the spiked pastes were promising, especially for B. The importance of matrix and environmental control on redox conditions was illustrated by the different behavior of Se-leachability when the spiking solution was selenite *vs.* selenate. The results are most immediately applicable to disposal of these materials in monofills. How the addition of hazardous waste liquids or solids to the CCBP in S/S technologies could affect the physical properties and leachabilities will have to be studied for each class of waste. The long-term durability issues discussed above apply also to the release rate of hazardous elements immobilized in sulfo-pozzolanic binders.

Acknowledgements

This research was supported by the Department of Energy and the Gas Research Institute, and by the sponsors of the Coal Ash Residuals Research Consortium (Northern States Power, Cooperative Power, Otter Tail Power, Contech Admixtures, Plains Pozzolanic) at the University of North Dakota and the North Dakota State University. J.A. Bender, J.E. Knell, M.C. Oseto, S.D. Adamek, C.M. Lillemoen and D.F. Pflughoeft-Hassett are thanked for technical assistance with portions of this study.

References

1. G.J. McCarthy, G.H. Groenewold, R.J. Stevenson, D.J. Hassett and K.H. Henke, in Fly Ash and Coal Conversion By-Products: Characterization, Utilization and Disposal II, Mat. Res. Soc. Symp. Proc. Vol. 65, 301 (1986).

2. P. Kumarathasan and G.J. McCarthy, in Fly Ash and Coal Conversion By-Products: Characterization, Utilization and Disposal III, Mater. Res. Soc. Symp. Proc. Vol. 86, 109 (1987).
3. D.J. Hassett and D.F. Hassett, in Fly Ash and Coal Conversion By-Products: Characterization, Utilization and Disposal IV, Mater. Res. Soc. Symp. Proc. Vol. 113, 333 (1988).
4. D.J. Hassett, D.F. Pflughoeft-Hassett, P. Kumarathasan and G.J. McCarthy, in Proc. 12th Ann. Madison Waste Conf. on Municipal and Industrial Waste, 471 (1989).
5. P. Kumarathasan, G.J. McCarthy, D.J. Hassett, and D.F. Pflughoeft-Hassett, in Fly Ash and Coal Conversion By-Products: Characterization, Utilization and Disposal VI, Mat. Res. Soc. Symp. Proc. Vol. 178, 83 (1990).
6. H. Pöllmann, H.J. Kuzel and R. Wenda. Neues Jahrbuch Miner. Abh., 160, 133 (1989).
7. H. Pöllmann, H.J. Kuzel and R. Wenda. Cem. Concr. Res., 20, 422 (1990).
8. H. Pöllmann, H.J. Kuzel and R. Wenda. Cem. Concr. Res., 20, 941 (1990).
9. D.J. Hassett, G.J. McCarthy, P. Kumarathasan and D.F. Pflughoeft-Hassett, Mater. Res. Bull. 25, 1347 (1990).
10. H. Pöllmann, H.-J. Kuzel and R. Wenda, Powder Diffraction File, International Centre for Diffraction Data, Newtown Square, PA, USA, pattern 41-217.
11. H. Pöllmann, St. Auer and H.-J. Kuzel, Cem. Concr. Res. 422 (1993).
12. P.L. Cote and T. Bridle. Waste Manage. Res., 5, 55 (1987).
13. P.L. Cote and T.W. Constable, Nucl. Chem. Waste Manage., 7 (1987).
14. D.L. Cocke, J. Hazard. Mater., 24:231 (1990).
15. R.J. Conner, Chemical Fixation and Solidification of Hazardous Wastes, Van Nostrand Reinhold, New York (1990).
16. A. Roy, H.C. Eaton, F.K. Cartledge and M.E. Tittlebaum, Hazard. Waste Hazard. Mater., 8, 33 (1991).
17. A. Roy, H.C. Eaton, F.K. Cartledge and M.E. Tittlebaum, Environ. Sci. Tech., 26, 1349 (1992).
18. G.J. McCarthy, D.J. Hassett and J.A. Bender, in Advanced Cementitious Systems, Mat. Res. Soc. Symp. Proc. Vol. 245, 129-140 (1992).
19. J.K. Solem and G.J. McCarthy, in Advanced Cementitious Systems, Mat. Res. Soc. Symp. Proc. Vol. 245, 71 (1992).
20. J.K. Solem-Tishmack, Use of Coal Conversion Solid Residuals in Solidification/Stabilization Technology. M.S. Thesis, Department of Soil Science, North Dakota State University, Fargo, ND, 173 pp. (1993).
21. G.J. McCarthy, J.K. Solem, O.E. Manz and D.J. Hassett, in Fly Ash and Coal Conversion By-Products: Characterization, Utilization and Disposal VI, Mat. Res. Soc. Symp. Proc. Vol. 178, 3 (1990).
22. American Society for Testing and Materials (ASTM). 1988. Annual Book of ASTM Standards. Section 4: Construction, Vol. 04.01: Cement, Lime, Gypsum.
23. G.J. McCarthy and A. Thedchanamoorthy, in Fly Ash and Coal Conversion By-Products: Characterization, Utilization and Disposal V, Mater. Res. Soc. Symp. Proc. Vol. 136 (1989).
24. Thedchanamoorthy, A. and G.J. McCarthy, Adv. X-Ray Anal., 32, 565 (1989).
25. J.A. Bender, J.K. Solem, G.J. McCarthy, M.C. Oseto and J.E. Knell, Adv. X-Ray Anal., 36, 343 (1993).
26. J.A. Bender, M.S. Thesis, Department of Chemistry, North Dakota State University, Fargo, ND, 105 pp. (1993).
27. G.J. McCarthy, J.A. Bender, J.K. Solem and K.E. Eylands, in Proc. Tenth Intern. Ash Use Symp., EPRI TR-101774s, Electric Power Research Institute, Polo Alto, CA, pp. 58/1-14 (1993).
28. U.S. Environmental Protection Agency, Handbook for Stabilization/Solidification of Hazardous Waste, No. 540/2-86/001, Cincinnati, OH, (1986); Federal Register, Vol. 51, No. 9, pp. 1750-1758 (1986).
29. D.F. Pflughoeft-Hassett, D.J. Hassett and C. M. Lillemoen, in Proc. Tenth Intern. Ash Use Symp., EPRI TR-101774s, Electric Power Research Institute, Polo Alto, CA, pp. 31/1-12 (1993). See also: D.J. Hassett, in Proceedings of the Waste Management for the Energy Industries Conference, University of North Dakota (1987).

30. E.E. Berry, R.T. Hemmings, and B.J. Cornelius, Commercialization Potential of AFBC Concrete: Part 2, Vol. 2: Mechanistic Basis for Cementing Action, Electric Power Research Institute, Palo Alto, CA, Project #2708-4, EPRI Report #GS-7122 (1991).
31. S. Mindness and J.F. Young, Concrete, Prentice-Hall, Inc., Englewood Cliffs, NJ (1981).
32. P.K. Mehta, Cem. Concr. Res., 3, 1 (1973).
33. P.K. Mehta, Cem. Concr. Res., 13, 401 (1983).
34. M.D. Cohen, Cem. Concr. Res., 13, 809 (1983).
35. X. Ping and J.J. Beaudoin, Cem. Concr. Res., 22, 631 (1992).
36. X. Ping and J.J. Beaudoin, Cem. Concr. Res., 22, 845 (1992).
37. Stabilization/Solidification of CERCLA and RCRA wastes. No. 625/6-89/022, Cincinnati, OH. (1989).
38. W.L. Stout, J.L. Hern, R.F. Korcak, and C.W. Carlson. Manual for Applying Fluidized Bed Combustion Residue to Agricultural Lands, Agricultural Research Service, ARS-74 (1988).
39. D. Damidot and F.P. Glasser, Cem. Concr. Res., 23, 221 (1993).
40. T. Grounds, H.G. Midgley and D.V. Nowell, Thermochim. Acta, 135, 347 (1988).
41. T. Nishikwa, K. Suzuki, S. Ito, K. Sato and T. Takebe, Cem. Concr. Res., 22, 6 (1993).
42. R.D. Butler, D.W. Brekke, H.J. Foster J. Solc and G.J. McCarthy, in Proc. Seventeenth Biennial Low-Rank Fuels Symposium, St. Louis, MO, Publ. by UND-Energy and Environmental Research Center, Grand Forks, ND, pp. 515-530 (1993).
43. G.J. McCarthy and J.K. Solem-Tishmack, in Advances in Cement and Concrete, Proc. Eng. Found. Conf., publ. by Am. Soc. Civil Engineers, pp. 103-121 (1994).
44. G.J. McCarthy, R.D. Butler, D.W. Brekke, S.D. Adamek, J.A. Parks, H.J. Foster, and J. Solc, in Microstructure in Cement-Based Systems, edited by S. Diamond, Mater. Res. Soc. Symp. Proc. (in press).